Available online at www.sciencedirect.com
ScienceDirect
Journal of Organometallic Chemistry 692 (2007) 234–242
Journal of Organometallic Chemistry
www.elsevier.com/locate/jorganchem

Zirconium complexes of the tridentate bis(aryloxide)-*N*-heterocyclic-carbene ligand: Chloride and alkyl functionalized derivatives

Dao Zhang, Hidenori Aihara, Takahito Watanabe, Tsukasa Matsuo, Hiroyuki Kawaguchi *

Coordination Chemistry Laboratories, Institute for Molecular Science, Myodaiji, Okazaki 444-8787, Japan

Received 23 February 2006; accepted 20 March 2006
Available online 30 August 2006

Abstract

The disodium salt of a bis(aryloxide)-*N*-heterocyclic-carbene dianionic ligand, $Na_2[L]$, was prepared by reaction of 1,3-bis(4,6-di-*tert*-butyl-2-hydroxybenzyl)imidazolium bromide $[H_3L]Br$ with 3 equiv. of $NaN(SiMe_3)_2$. Reaction of $ZrCl_4(thf)_2$ with 1 equiv. of $Na_2[L]$ gave a mixture of $[L]ZrCl_2(thf)$ (**1**) and $[L]_2Zr$ (**2**). When the amount of $Na_2[L]$ was increased to 2 equiv., the bis(bis(aryloxide)-*N*-heterocyclic-carbene) complex **2** was obtained in good yield. The dichloro complex **1** is a precursor to organometallic derivatives, and treatment with $PhCH_2MgCl$ or Me_3SiCH_2Li yielded $[L]ZrR_2$ [$R = CH_2Ph$ (**3**), CH_2SiMe_3 (**4**)]. The disodium salt of the ligand $Na_2[L]$ is unstable and undergoes 1,2-benzyl migration, whereas zirconium complexes of the $[L]^{2-}$ ligand are found to be thermally stable in solid and solution. The X-ray crystal structures of **1**, **2**, and **3** are described.

Keywords: Zirconium; Carbene; Aryloxide; Multidentate ligand

1. Introduction

The chemistry and application of *N*-heterocyclic carbenes (NHCs) have been extensively explored [1]. They can bind as two-electron donors to a wide range of transition metal, main group, and f-block derivatives [2]. Especially, NHCs have been found extensive use as ancillary ligands in late transition metal complexes, in which they have shown enhanced catalytic activity compared to their phosphine analogues [1,3]. These improved catalytic systems have been attributed to the robust nature of late transition metal–NHC bond and their excellent σ-donating properties [4]. In contrast, NHC complexes of early transition metals are considerably less developed despite the great potential of this class of molecules [5,6]. This is mainly due to the ease of dissociation of the NHC ligand from the electron deficient metal center, which makes it difficult to study the chemistry of NHCs in early transition metals and f-elements [7]. A potential means of directing metal–NHC interactions is the covalent tethering of the anionic functional groups to the NHC ligand system, where the NHC moiety is held in proximity of the metal center by a covalent tether and should affect reactivity in a specific way. Recent examples include amide-, alkoxide-, and cyclopentadienyl-functionalized NHC ligands [7–10]. As part of an ongoing project to study the chemistry of aryloxide-based multidentate ligands [11], we have successfully used the tridentate dianionic bis(aryloxide)–NHC ligand ($[L]^{2-}$) as an ancillary ligand to access NHC complexes of titanium. These compounds are found to be highly active procatalysts for polymerization of ethylene [12]. We therefore wish to extend this chemistry to early transition metals and synthesize a range of $[L]^{2-}$ supported zirconium complexes.

* Corresponding author.
E-mail address: hkawa@ims.ac.jp (H. Kawaguchi).

0022-328X/$ - see front matter © 2006 Elsevier B.V. All rights reserved.
doi:10.1016/j.jorganchem.2006.03.044

2. Results and discussion

2.1. Synthesis of $[H_3L]Br$

The proligand, 1,3-bis(4,6-di-*tert*-butyl-2-hydroxybenzyl)-imidazolium bromide $H_3[L]Br$, was prepared by stepwise alkylation on the nitrogen atoms of imidazole using 2-bromomethyl-4,6-di-*tert*-butylphenol (Scheme 1). Reaction of imidazole with 2-bromomethyl-phenol in the presence of $NaHCO_3$ in refluxing THF gave *N*-(2-hydroxybenzyl)imidazole as a colorless solid in 96% yield. Subsequent treatment of it with 2-bromomethyl-phenol in THF yielded $H_3[L]Br$ as colorless microcrystals in 63%. The most prominent features of the ^1H and ^{13}C NMR spectra of $H_3[L]Br$ are the resonances for the imidazolium proton at 9.51 ppm and the corresponding imidazolium carbon at 139.1 ppm.

The molecular structure of $H_3[L]Br$ was determined by X-ray analysis (Fig. 1). Recrystallization from DME gave single crystals of $H_3[L]Br \cdot DME$. Hydrogen atoms attached to imidazolium carbon and oxygen atoms were located from the different Fourier map and were refined isotropically. The molecule adopts an S-shaped conformation. Of interest is the incorporation of a DME molecule of crystallization held in place through a hydrogen bond between the imidazolium proton [H(3)] and one of the oxygen atoms of DME [O(3)] (C–H···O, 2.62 Å, 136°). Each $H_3[L]$ unit is connected to another unit through hydrogen bonds between bromide ions and hydroxyl groups [O(1)–H(1)···Br, 2.39 Å, 171°; O(2)–H(2)···Br*, 2.50 Å, 165°] [13], giving a dimeric structure in the solid state.

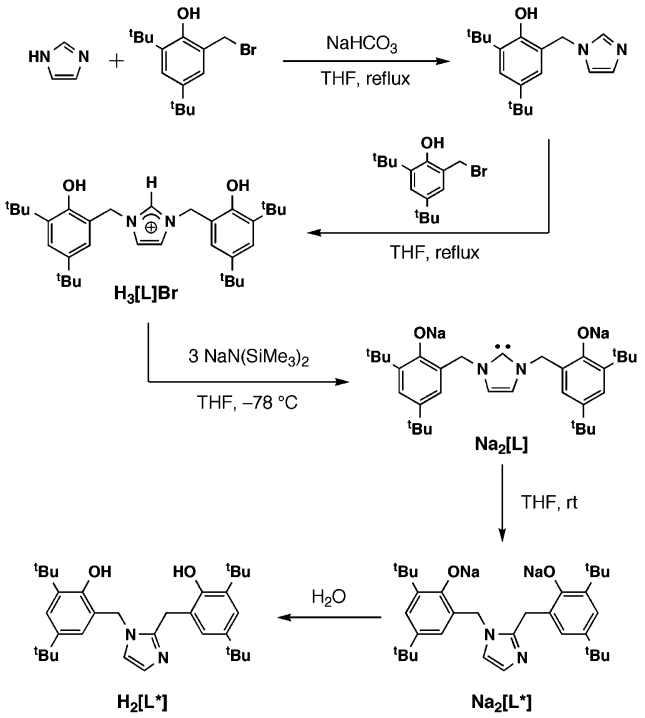

Scheme 1.

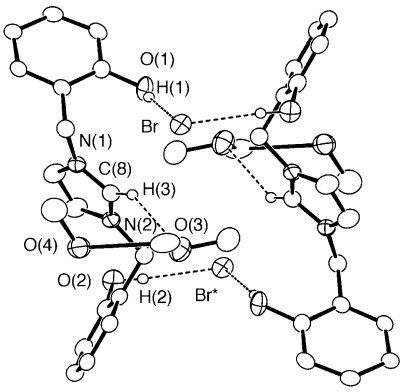

Fig. 1. The molecular structure of $H_3[L]Br$. ^{t}Bu groups and hydrogen atoms except for the hydroxyl and imidazolium protons are omitted for clarity.

We examined deprotonation of $H_3[L]Br$ to prepare alkali metal salts of the ligand for use in subsequent salt metathesis with metal halides. The sodium salt $Na_2[L]$ was readily prepared by the reaction of $H_3[L]Br$ with 3 equiv. of $NaN(SiMe_3)_2$ in THF at −78 °C. However, attempts to isolate $Na_2[L]$ met with difficulties because of its thermal instability. The facile 1,2-benzyl migration took place at ambient temperature, giving a 2-alkylated imidazole derivative $Na_2[L^*]$ (Scheme 1). This type of 1,2-migration is a common reaction for singlet carbenes [9,14]. The X-ray diffraction analysis shows it to be the dimeric complex $\{Na_2[L^*]\}_2$ (Fig. 2). The dimer resides on a crystallographic C_2-axis; its core consists of two four-membered Na_2O_2 rings. Hydrolysis of $Na_2[L^*]$ afforded 1,2-bis(2-hydroxybenzyl)imidazole $H_2[L^*]$, which was characterized by NMR spectroscopy and X-ray crystallography (Fig. 3).

As shown later, the proligand $H_3[L]Br$ itself can be used directly in reaction with transition metal complexes, but it is clearly advantageous to have in hand sodium derivatives, too, for use via salt elimination reactions. Fortunately, the sodium salt $Na_2[L]$ obtained from the reaction between $H_3[L]Br$ and $NaN(SiMe_3)_2$ is sufficient clean to be used without additional purification.

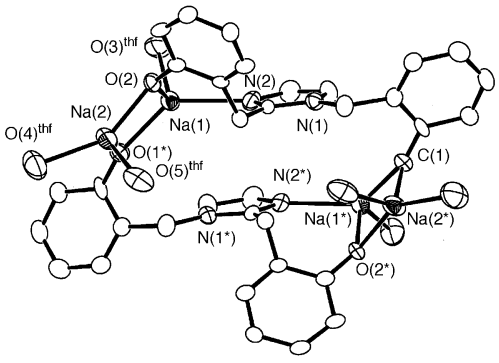

Fig. 2. The molecular structure of $Na_2[L^*]$. ^{t}Bu groups, carbon atoms of THF, and hydrogen atoms are omitted for clarity.

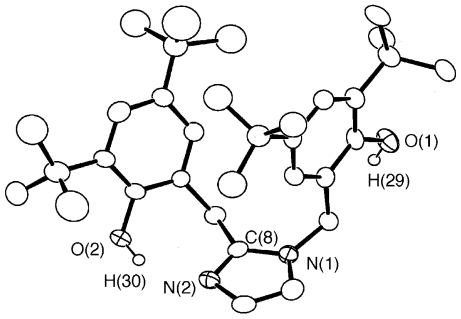

Fig. 3. The molecular structure of $H_2[L^*]$. Hydrogen atoms except for the hydroxyl protons are omitted for clarity.

2.2. Synthesis of $Zr(L)Cl_2(thf)$ (1) and $Zr(L)_2$ (2)

Treatment of $ZrCl_4(thf)_2$ with 1 equiv. of freshly prepared $Na_2[L]$ in THF at −78 °C afforded the mono-ligand complex $[L]ZrCl_2(thf)$ (**1**) as well as the bis-ligand complex $[L]_2Zr$ (**2**) (Scheme 2). Different solubility properties of **1** and **2** allowed us to separate them. Recrystallization of the products from toluene/hexane resulted in colorless crystals of **1** in 20% yield, and **2** could be crystallized as light yellow crystals from THF/hexane in 38% yield. The latter could also be synthesized in 84% yield by the reaction of $ZrCl_4(thf)_2$ with 2 equiv. of $Na_2[L]$ in THF, while attempts to prepare the desirable mono-ligand complex **1** in high yield have been unsuccessful. The isolated complexes **1** and **2** are stable in solution, and **1** is not found to generate **2** via ligand redistribution on prolong standing in $CDCl_3$ according to NMR spectroscopy. Previously, we found that the analogous (1:1) $TiCl_4(thf)_2/Na_2[L]$ reaction

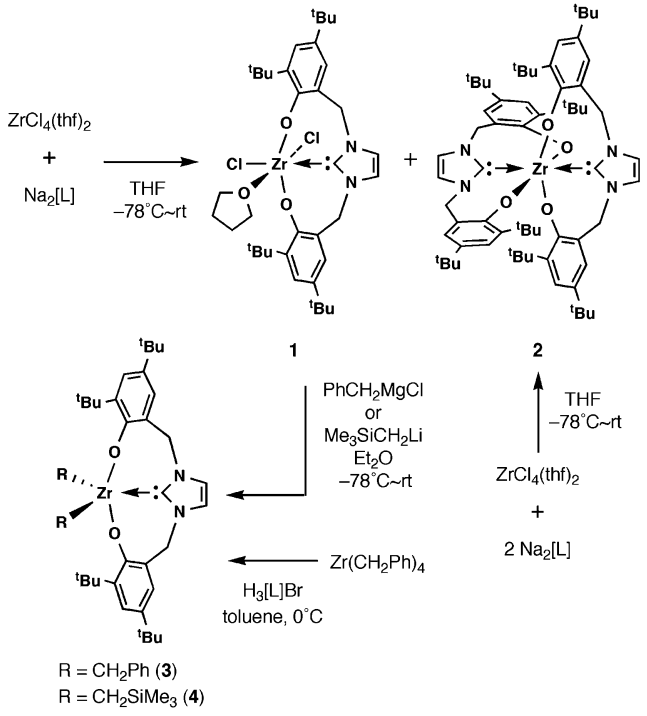

Scheme 2.

afforded the mono-ligand complex as the sole isolable product in 74% yield [12]. The large ionic radius of zirconium relative to titanium may enable facile formation of the bis-ligand complex **2**. Complexes **1** and **2** were characterized by NMR data and X-ray analysis.

The molecular structure of **1** is shown in Fig. 4, together with relevant bond distances and angles. The structure is similar to the titanium derivative, $[L]TiCl_2(thf)$ [12]. Compound **1** displays a distorted octahedral geometry at zirconium, in which the aryloxide units of the meridionally coordinated $[L]^{2-}$ ligand occupy the axial positions. These are considerably disordered from idealized geometry by approximately 17° [O(1)–Zr–O(2), 162.5(3)°]. The bis-(aryloxide)–NHC ligand assumes an S-shaped conformation with the dihedral angle of 33.3(4)° between ZrC(8)N(1)N(2) and ZrC(8)O(1)O(2) planes, a well-established structural feature of this ligand set. The two chloride atoms adopt a mutually *cis* disposition, and a THF molecule is *trans* to one of the chloride ligands. The metal–carbene distance of **1** [2.35(1) Å] is somewhat shorter than those of the known Zr(IV)–NHC complexes [2.391(5)–2.456(3) Å] [8e,15]. This decrease reflects geometrical constrains arising from strain in the tridentate bis-(aryloxide)–NHC system. The two Zr–Cl bonds are alike [2.450(3) and 2.445(3) Å]. It should be noted that the NHC moiety of the $[L]^{2-}$ ligand has *trans* influence comparable to that of THF, although the strong donating properties of NHCs are generally emphasized.

The temperature-dependent NMR spectroscopic features of **1** are complex. The room temperature ^1H NMR spectrum of **1** in $CDCl_3$ shows two broad signals of the $N–CH_2$ protons at 3.73 and 6.52 ppm. Below 273 K, the $N–CH_2$ protons give rise to one set of mutually coupled doublets at 4.43 and 6.39 ppm as well as two sets of mutually coupled doublets at 4.4, 4.6, 5.2, and 6.3 ppm. As the temperature is lowered to 223 K, the signals of the ^1H NMR spectra gradually sharpen and the latter sets of signals increase in intensity relative to the other.

The two sets of mutually coupled doublets at 4.4, 4.6, 5.2, and 6.3 ppm at low temperature can be assigned to a molecular structure with C_1 symmetry found in the solid

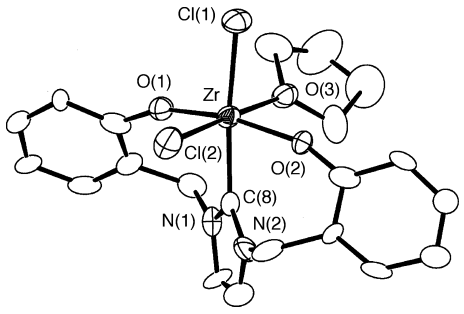

Fig. 4. The molecular structure of **1**. ^{t}Bu groups and hydrogen atoms are omitted for clarity. Selected bond distances (Å) and angles (°): Zr–C(8) 2.35(1), Zr–O(1) 1.995(8), Zr–O(2) 1.986(7), Zr–O(3) 2.262(8), Zr–Cl(1) 2.450(3), Zr–Cl(2) 2.445(3); O(1)–Zr–O(2) 162.5(3), Cl(1)–Zr–C(8) 169.5(3), Cl(1)–Zr–O(3) 85.3(2), Cl(1)–Zr–Cl(2) 96.8(1).

state (isomer **A**, in Scheme 3), as its ^{1}H NMR spectrum shows well-defined peaks in an overall pattern that resembles closely that of the titanium derivative [L]TiCl$_2$(thf) [12]. The other pair of doublets of the N–CH$_2$ protons evidently belongs to another single isomer with higher symmetry (**B**). Below room temperature, the THF protons appear as four distinct signals, although no fine structure is observed, suggesting that the THF is coordinated to the metal in each isomer **A** and **B**. The ^{1}H NMR spectrum of the isomer **B** is consistent with the molecule possessing effective C_2 symmetry, in which the THF molecule is positioned *trans* to the NHC carbene carbon with a twofold axis passing through the Zr metal center, the THF oxygen, and the carbene of the S-shaped ligand. Although we have yet to find that the tridentate bis(aryloxide)–NHC ligand adopts a U-shaped conformation, the current results do not conclusively rule out an alternative isomer with C_s symmetry (**B′**).

It is apparent from the ^{1}H NMR spectral data that the two isomers **A** and **B** are in equilibrium (Scheme 3). This is also supported by variable temperature ^{13}C NMR spectroscopy. For example, the NHC carbene carbon is observed as one weak signal (183.5 ppm) at room temperature and gives rise to two signals (182.5 and 183.0 ppm) at lower temperature (243 K). The broadened resonances in the NMR spectra for this system arise, because the equilibrium process that interconverts these species occurs at a rate that is comparable to the NMR time scale. We suggest that the dissociation/re-coordination of THF occurs in solution. This could give a five-coordinate intermediate through which one chloride and the THF group could exchange positions. To evaluate the equilibrium between **A** and **B**, the concentration of each species was measured at separate temperatures, for which reliable measurements could be made from integration of the ^{1}H NMR spectra. Equilibrium constants were calculated according to $K = [\mathbf{A}]/[\mathbf{B}]$ and plotted as a function of temperature. The thermodynamic parameters obtained by the van't Hoff plot show that the isomer **A** is preferred over the isomer **B** on enthalpic terms ($\Delta H^\circ = -8.0$ kJ mol^{-1}), but the equilibrium is disfavored entropically ($\Delta S^\circ = -31$ J mol^{-1} K^{-1}). There may be steric interactions between the *tert*-butyl groups and the THF molecule *cis* to the NHC carbene carbon in a structure for **A**, resulting in lowered mobility of the *tert*-butyl groups or THF.

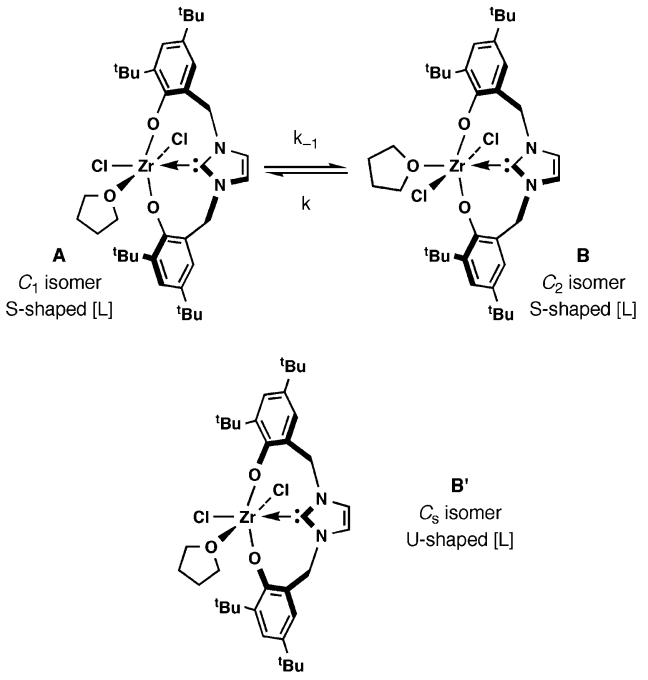

Scheme 3.

The molecular structure of the bis-ligand complex **2** is depicted in Fig. 5, together with relevant bond distances and angles. The zirconium center shows a distorted octahedral geometry and features two meridionally coordinated tridentate [L]$^{2-}$ ligands, each with mutually *trans* NHC carbene donors [C(8)–Zr–C(41), 160.35(7)°]. The molecule has approximate C_2 symmetry. The ligands adopt an S-shaped conformation again, and the twisted angles of the ligands [ZrC(8)N(1)N(2)/ZrC(8)O(1)O(2), 32.48(8)°; ZrC(41)N(3)N(4)/ZrC(41)O(3)O(4), 33.51(9)°] are similar to that of **1**. The dihedral angle between two NHC rings is 18.1(1)°. The Zr–C(carbene) [2.383(3) and 2.380(3) Å] and Zr–O(aryloxide) distances [average 2.075 Å] are comparable to the corresponding distances found in **1**. The NMR data of **2** are consistent with the solid state structure, and signals for only a single D_2 symmetric bis(bis(aryloxide)–NHC) ligand environment are seen, although the slight broadening of signals assigned to the N–CH$_2$ protons at 4.41 and 6.08 ppm indicates some fluxional process at room temperature. The *tert*-butyl groups appear as two singlets at 0.87 and 1.23 ppm, and the NHC ring protons are observed as a singlet at 7.05 ppm. In the room temperature ^{13}C NMR spectrum, the NHC carbene carbon is observed at 185.5 ppm.

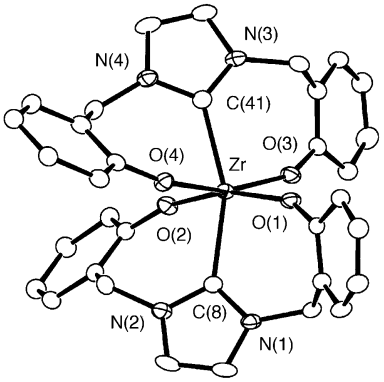

Fig. 5. The molecular structure of **2**. ^{t}Bu groups and hydrogen atoms are omitted for clarity. Selected bond distances (Å) and angles (°): Zr–C(8) 2.383(3), Zr–C(41) 2.380(3), Zr–O(1) 2.027(1), Zr–O(2) 2.039(2), Zr–O(3) 2.018(2), Zr–O(4) 2.034(2); C(8)–Zr–C(41) 160.35(7), O(1)–Zr–O(2) 161.73(7), O(3)–Zr–O(4) 160.93(8).

2.3. Synthesis of [L]Zr(CH_2Ph)$_2$ (3) and [L]Zr(CH_2SiMe_3)$_2$ (4)

The successful isolation of **1** prompted us to examine substitution reactions of the chloride ligands (Scheme 2). Addition of 2 equiv. of $PhCH_2MgCl$ to **1** in Et_2O at −78 °C followed by standard workup afforded [L]Zr(CH_2Ph)$_2$ (**3**) as light yellow crystals in 48% yield. The analogous reaction using Me_3SiCH_2Li produced [L]Zr(CH_2SiMe_3)$_2$ (**4**) in 33%. We also examined the protonolysis of Zr(CH_2Ph)$_4$ with [H_3L]Br in toluene, but the reaction did not lead to the expected product [L]ZrBr(CH_2Ph). Instead, the dibenzyl complex **3** was obtained in 20% isolated yield. Ligand redistribution processes would complicate the reaction pathways. The formulas of alkyl derivatives **3** and **4** were inferred by NMR spectroscopy and elemental analysis, and the molecular structure of **3** was determined by X-ray crystallography.

The molecular structure of **3** is shown in Fig. 6, together with relevant bond distances and angles. The structure of **3** is similar to that of the titanium derivative [L]Ti(CH_2Ph)$_2$ [4]. The geometry at zirconium is distorted trigonal bipyramidal with a meridional coordination of the tridentate $[L]^{2-}$ ligand. The two aryloxide donors [O(1) and O(2)] occupy the axial positions with the O–Zr–O angle of 160.84(9)°. The twist angle of the S-shaped ligand in **3** [40.1(1)°, ZrC(8)N(1)N(2)/ZrC(8)O(1)O(2)] is larger than those of **1** and **2**. The Zr–C(carbene) distance [2.309(3) Å] is shortened relative to those of the six-coordinated NHC complexes **1** and **2**. The Zr–C_α–C_{ipso} angles of 109.1(2)° and 118.9(2)° indicate η^1 binding of the benzyl groups, and the Zr–C(benzyl) distances of 2.264(4) and 2.247(3) Å are normal [16].

The NMR data of **3** and **4** show C_2 symmetry in solution, and the structure of **3** is more fluxional in solution than that of **4**. The room temperature ^{13}C NMR spectra of **3** and **4** exhibit a NHC carbene signal at 187.5 and 185.8 ppm. In the room temperature ^1H NMR spectrum of **3** in C_6D_6, two signals of *tert*-butyl groups appear at 1.36 and 1.87 ppm. The N–CH_2 and Zr–CH_2 protons are observed as four broad signals at 2.81, 3.26, 3.53 and 3.71 ppm due to a fluxional process. We performed variable-temperature NMR studies to explore the dynamic behavior of **3** in C_7D_8. As an NMR sample is cooled, the N–CH_2 and Zr–CH_2 protons give two sets of mutually coupled doublets. The ^1H NMR line shape analysis for these signals gives the following activation parameters for the atropisomerization: $\Delta H^\ddagger = 62.1$ kJ mol^{-1}; $\Delta S^\ddagger = -8.2$ J mol^{-1} K^{-1}, which are comparable to those of isostructural Ti(L)(CH_2Ph)$_2$ [$\Delta H^\ddagger = 64.8$ kJ mol^{-1}; $\Delta S^\ddagger = -6.2$ J mol^{-1} K^{-1}] [12]. The small magnitude of $\Delta S^\ddagger$ is in accord with a nondissociative rearrangement [17]. For **4**, the room temperature ^1H NMR spectrum exhibits two sets of mutually coupled doublets assignable to the N–CH_2 and Zr–CH_2 protons. The encumbering alkyl groups may hamper atropisomerization of **4**.

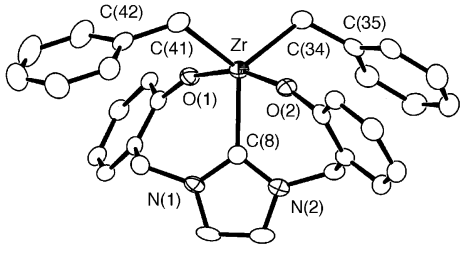

Fig. 6. The molecular structure of **3**. ^{t}Bu groups and hydrogen atoms are omitted for clarity. Selected bond distances (Å) and angles (°): Zr–C(8) 2.309(3), Zr–C(34) 2.264(4), Zr–C(41) 2.247(3), Zr–O(1) 2.011(2), Zr–O(2) 1.992(2); O(1)–Zr–O(2) 160.84(9), C(8)–Zr–C(34) 125.3(1), C(8)–Zr–C(41) 126.1(1), C(34)–Zr–C(41) 108.6(1), Zr–C(34)–C(35) 109.1(2), Zr–C(41)–C(42) 118.9(2).

3. Conclusion

This investigation into zirconium *N*-heterocyclic carbene chemistry has focused on the chelating bis(aryloxide)–NHC ligand $[L]^{2-}$, which is readily prepared in high yield. Reaction of $ZrCl_4(thf)_2$ with Na_2[L] resulted in a mixture of [L]$ZrCl_2$(thf) (**1**) and [L]$_2$Zr (**2**). Their X-ray structures showed the meridional coordination manner of the tridentate $[L]^{2-}$ ligand with an S-shaped conformation. The complex **1** proved to be a versatile precursor to organometallic complexes via chloride displacement reactions with $PhCH_2MgCl$ and Me_3SiCH_2Li, giving the corresponding alkyl derivatives [L]ZrR_2 (R = CH_2Ph (**3**), CH_2SiMe_3 (**4**)). During the alkylating reactions, the S-shaped conformation of the $[L]^{2-}$ ligand is retained. Coupled with the NMR data, the short Zr–NHC distances of **1**, **2** and **3** suggest that the NHC carbene carbon is strongly bound to the zirconium metal. Compounds **1**, **3**, and **4** should provide excellent starting materials for investigation of the reactivity of this class of group 4 metal complexes. We expect it to demonstrate a rich and varied chemistry.

4. Experimental

4.1. General methods

All manipulations of air- and/or moisture-sensitive compounds were performed under argon atmosphere using standard Schlenk-line techniques and a glove-box (MBraun Labmaster 130) filled with dinitrogen (<1 ppm H_2O/O_2). All dried, oxygen-free solvents and chemicals commercially available were used as received without further purification. Deuterated benzene (C_6D_6) was dried and degassed over a potassium mirror in vacuo prior to use. Deuterated chloroform ($CDCl_3$) was distilled from calcium hydride prior to use. NMR measurements were carried out on JEOL Lambda-500, JNM-GX500, and LA-400 spectrometers. Chemical shifts (δ) for ^1H NMR spectra were referenced to residual protic solvents peaks (residual C_6D_5H in C_6D_6, $^1H(\delta) = 7.15$; residual $CHCl_3$ in $CDCl_3$, $^1H(\delta) = 7.24$). Elemental analyses (C, H, and N) were measured using YANACO MT-6 and MSU-32 microanalyzers.

4.2. Synthesis

4.2.1. N-(4,6-Di-tert-butyl-2-hydroxybenzyl)imidazole

A flask was charged with imidazole (4.8 g, 70 mmol), anhydrous sodium bicarbonate ($NaHCO_3$, 6.2 g, 74 mmol), and THF (50 mL). A solution of 2-bromomethyl-4,6-di-*tert*-butylphenol (20 g, 67 mmol) in THF (100 mL) was slowly added to the mixture at reflux temperature. After stirring for 12 h, the mixture was poured into water, and the product was extracted with Et_2O. The combined organic layers were dried over Na_2CO_3 and then volatiles were removed in vauo to give an off-white solid. Crystallization of the crude product from Et_2O/hexane gave a colorless crystalline solid of *N*-(4,6-di-*tert*-butyl-2-hydroxybenzyl)imidazole (18.3 g, 96%).

Elemental analysis. Calc. for $C_{18}H_{28}N_2O$: C, 75.48; H, 9.15; N, 9.78. Found: C, 74.48; H, 9.07; N, 9.69%. ^1H NMR ($CDCl_3$, 298 K): $\delta = 1.30$ (s, 9H, ^{t}Bu), 1.66 (s, 9H, ^{t}Bu), 2.56 (s, 2H, CH_2), 6.35 (s, 1H), 6.63 (s, 1H), 6.71 (s, 1H), 6.35 (s, 1H), 6.91 (d, $J = 2.4$ Hz, 1H, ArH), 7.58 (d, $J = 2.4$ Hz, 1H, ArH).

4.2.2. H_3[L]Br

A flask was charged with *N*-(4,6-di-*tert*-butyl-2-hydroxybenzyl)imidazole (10.0 g, 35 mmol) and THF (25 mL). A solution of 2-bromomethyl-4,6-di-*tert*-butylphenol (9.0 g, 30 mmol) in THF (50 mL) was slowly added at reflux temperature. After stirring for 12 h, the solution was evaporated to dryness to give the crude product. The product was washed with toluene and hexane, and dried in vacuo, which yielded colorless microcrystals of $[H_3L]Br$ (11.0 g, 63%).

Elemental analysis. Calc. for $C_{33}H_{49}N_2O_2Br$: C, 67.68; H, 8.43; N, 4.78. Found: C, 67.39; H, 8.41; N, 4.74%. ^1H NMR ($CDCl_3$, 298 K): $\delta = 1.25$ (s, 18H, ^{t}Bu), 1.38 (s, 18H, ^{t}Bu), 5.53 (s, 4H, CH_2), 6.95 (br.s, 2H, OH), 7.07 (d, $J = 2.4$ Hz, 2H, ArH), 7.12 (d, $J = 1.2$ Hz, 2H, CH), 7.32 (d, $J = 2.4$ Hz, 2H, ArH), 9.51 (br.s, 1H, CH); $^{13}C\{^1H\}$ NMR ($CDCl_3$, 298 K): $\delta = 30.3$ (C*C*H$_3$), 31.7 (C*C*H$_3$), 34.5 (*C*CH$_3$), 35.1 (*C*CH$_3$), 51.3 (CH_2), 122.3 (C), 121.4 (CH), 125.3 (CH), 125.7 (CH), 136.0 (C), 139.1 (CH, imidazolium C2), 143.4 (C), 151.4 (C).

4.2.3. 1,2-Bis(4,6-di-tert-butyl-2-hydroxybenzyl)imidazole (H_2[L*])

A THF solution of $NaN(SiMe_3)_2$ (1.0 M, 15.4 mL, 15.4 mmol) was added to a suspension of $[H_3L]Br$ (3.0 g, 5.12 mmol) in THF (50 mL) at −78 °C. The mixture was allowed to warm up to room temperature and stirred for further 3 h. Then the mixture was poured into water and extracted with Et_2O. The combined organic layers were evaporated to dryness, and the residue was crystallized from Et_2O/hexane to give 1,2-disubstituted imidazole (H_2L^*) as colorless crystals.

Elemental analysis. Calc. for $C_{33}H_{48}N_2O_2$: C, 78.53; H, 9.59; N, 5.55. Found: C, 78.41; H, 9.67; N, 5.55%. ^1H NMR ($CDCl_3$, 298 K): $\delta = 1.15$ (s, 9H, ^{t}Bu), 1.21 (s, 9H, ^{t}Bu), 1.42 (s, 9H, ^{t}Bu), 1.43 (s, 9H, ^{t}Bu), 4.01 (s, 2H, CH_2), 5.16 (s, 2H, CH_2), 6.60 (d, $J = 2.4$ Hz, 1H, ArH), 6.73 (d, $J = 1.5$ Hz, 1H, CH), 6.83 (d, $J = 2.4$ Hz, 1H, ArH), 6.91 (d, $J = 1.5$ Hz, 1H, CH), 7.18 (d, $J = 2.4$ Hz, 1H, ArH), 7.23 (d, $J = 2.4$ Hz, 1H, ArH). The proton signals of the hydroxyl groups were not observed due to broadening.

4.2.4. Reaction of $ZrCl_4(thf)_2$ with Na_2[L]

A THF solution of $NaN(SiMe_3)_2$ (1.0 M, 9.9 mL, 9.9 mmol) was added to a suspension of $[H_3L]Br$ (1.93 g, 3.30 mmol) in THF (50 mL) at −78 °C. The ligand solution was cannulated into a THF (50 mL) solution of $ZrCl_4(thf)_2$ (1.25 g, 3.30 mmol) keeping the temperature below −78 °C. The mixture was allowed to warm to ambient temperature and stirred for further 6 h. After removal of volatiles in vacuo, the residue was extracted with toluene (50 mL) and centrifuged to remove insoluble materials. The resulting supernatant was concentrated by evaporation. Then the solution (10 mL) was layered with hexane (30 mL) and cooled to −30 °C to give $[L]ZrCl_2(thf)$ (**1**) as colorless plates (0.49 g, 20%). The mother liquid was evaporated to dryness, and the light yellow residue was extracted with hexane (30 mL × 3). The combined extracts were evaporated to dryness to leave a yellow residue, and recrystallization from THF/hexane afforded 1.37 g of $[L]_2Zr$ (**2**) as light yellow crystals in 38% yield. Crystals of **1** were contaminated with a small amount of **2**, which we could not separate by any method. Consequently we were unable accurate CNH microanalysis that could be unambiguously interpreted.

Complex ***1***: ^1H NMR (C_6D_6, 298 K): $\delta = 1.25$ (br.s, 4H, THF), 1.40 (s, 18H, ^{t}Bu), 1.82 (s, 18H, ^{t}Bu), 3.73 (br.s, 2H, CH_2), 4.39 (br.s, 4H, THF), 5.69 (s, 2H, CH), 6.52 (br.s, 2H, CH_2), 6.98 (s, 2H, ArH), 7.62 (s, 2H, ArH); $^{13}C\{^1H\}$ NMR ($CDCl_3$, 298 K): $\delta = 30.8$ (C*C*H$_3$), 31.6 (C*C*H$_3$), 34.2 (*C*CH$_3$), 35.4 (*C*CH$_3$), 54.2 (CH_2), 120.1 (NCH), 124.9 (CH), 125.3 (CH), 141.5 (C), 159.2 (C), 183.5 (C, carbene). Several signals are broadened and/or overlapped in aromatic region, and signals of THF are broadened at room temperature.

Complex ***2***: Elemental analysis. Calc. for $C_{66}H_{94}N_4O_4Zr$: C, 72.15; H, 8.62; N, 5.10. Found: C, 71.78; H, 8.23; N, 4.17%. ^1H NMR ($CDCl_3$, 298 K): $\delta = 0.87$ (s, 36H, ^{t}Bu), 1.23 (s, 36H, ^{t}Bu), 4.41 (br.s, 4H, CH_2), 6.08 (br.s, 4H, CH_2), 6.96 (s, 4H, ArH), 7.05 (s, 4H, CH), 7.08 (s, 4H, ArH); $^{13}C\{^1H\}$ NMR ($CDCl_3$, 298 K): $\delta = 30.4$ (C*C*H$_3$), 31.8 (C*C*H$_3$), 34.1 (*C*CH$_3$), 34.9 (*C*CH$_3$), 53.7 (CH_2), 119.5 (NCH), 123.1 (CH), 123.7 (CH), 124.4(C), 136.2 (C), 138.1 (C), 160.9 (C), 185.5 (C, carbene).

4.2.5. Analysis of the equilibrium of *1* in solution

Complex **1** was dissolved in $CDCl_3$, and the tube was sealed under an argon atmosphere. ^1H NMR spectra were taken at 9 temperatures ranging from 223 to 263 K. The *K* values obtained at given temperature are as follows: 223 K,

1.788; 228 K, 1.622; 233 K, 1.480; 238 K, 1.388; 243 K, 1.282; 248 K, 1.176; 253 K, 1.080; 258 K, 0.990; 263 K, 0.930. Thermodynamic parameters were determined from van't Hoff plots of the above data.

4.2.6. [L]$_2$Zr (2)

A THF solution of $NaN(SiMe_3)_2$ (1.0 M, 3.3 mL, 3.3 mmol) was added to a suspension of $[H_3L]Br$ (0.59 g, 1.00 mmol) in THF (20 mL) at −78 °C. The ligand solution was cannulated into a THF (20 mL) solution of $ZrCl_4(thf)_2$ (0.19 g, 0.50 mmol) keeping the temperature below −78 °C. The mixture was allowed to warm to ambient temperature and stirred for further 12 h. After removal of volatiles in vacuo, the residue was extracted from hexane (50 mL) and centrifuged to remove insoluble materials. The extract was evaporated to dryness. Recrystallization from THF/hexane gave **2** as light yellow crystals (0.92 g, 84%).

4.2.7. [L]Zr(CH_2Ph)$_2$ (3): reaction of 1 and $PhCH_2MgCl$

An Et_2O solution of $PhCH_2MgCl$ (1.0 M, 1.1 mL, 1.1 mmol) was added to **1** (0.40 g, 0.54 mmol) in Et_2O (40 mL) at −78 °C. The mixture was allowed to warm up to ambient temperature and stirred for further 10 h. After removal of the solvent under reduced pressure, the light yellow residue was extracted with Et_2O (30 mL) and centrifuged to remove insoluble material. The supernatant was evaporated to dryness, and then the residue was crystallized from Et_2O/hexane to afford **3** as light yellow crystals (198 mg, 48%).

Elemental analysis. Calc. for $C_{47}H_{61}N_2O_2Zr$: C, 72.63; H, 7.91; N, 3.60. Found: C, 72.05; H, 8.05; N, 3.62%. ^{1}H NMR (C_6D_6, 298 K): $\delta = 1.36$ (s, 18H, ^{t}Bu), 1.87 (s, 18H, ^{t}Bu), 2.81 (br.s, 2H, CH_2), 3.26 (br.s, 2H, CH_2), 3.53 (br.s, 2H, CH_2), 3.71 (br.s, 2H, CH_2), 5.53 (s, 2H, CH), 6.74 (t, $J = 8$ Hz, 2H, benzyl(*para*)), 6.88 (d, $J = 3$ Hz, 2H, ArH), 6.89 (dd, $J = 8$ Hz, 4H, benzyl(*meta*)), 7.16 (d, $J = 8$ Hz, 4H, benzyl(*ortho*)), 7.62 (d, $J = 3$ Hz, 2H, ArH); ^{13}C{^{1}H} NMR (C_6D_6, 298 K): $\delta = 32.0$ (CCH_3), 32.9 (CCH_3), 35.3 (CCH_3), 36.9 (CCH_3), 53.7 (CH_2), 67.5 (CH_2), 119.5 (NCH), 122.1(CH), 125.1 (CH), 125.3 (CH), 126.9 (C), 127.8 (CH), 129.2(CH), 138.5 (C), 141.0 (C), 143.9 (C), 160.1 (C), 187.5 (C, carbene).

4.2.8. [L]Zr(CH_2Ph)$_2$ (3): reaction of Zr(CH_2Ph)$_4$ with H_3[L]Br

A suspension of H_3[L]Br (950 mg, 1.62 mmol) in toluene (65 mL) was added to $Zr(CH_2Ph)_4$ (746 mg, 1.64 mmol) in toluene (20 mL) at 0 °C. The mixture was stirred for further 4 h at ambient temperature. Volatiles were removed in vacuo to leave a light yellow residue. The residue was washed with Et_2O/hexane (30 mL/20 mL) and dried in vacuo, yielding a yellow solid of **3** (256 mg, 20%).

4.2.9. Analysis of the fluxionality of 3 in solution

Complex **3** was dissolved in toluene-d_8, and the tube was sealed under an argon atmosphere. ^{1}H NMR spectra were taken at eight temperatures ranging from 25 to 100 °C. Line shape analysis of the methylene region was carried out at each temperature using a GNMR program [18]. The k_1 values obtained at given temperature are as follows: 298 K, 32; 313 K, 100; 323 K, 240; 333 K, 410; 343 K, 900; 353 K, 1900; 363 K, 3500; 373 K, 6000. Activation parameters were determined from Eyring plots of the above data.

4.2.10. [L]Zr(CH_2SiMe_3)$_2$ (4)

A pentane solution of Me_3SiCH_2Li (1.0 M, 1.1 mL, 1.1 mmol) was added to **1** (0.40 g, 0.54 mmol) in Et_2O (40 mL) at −78 °C. The mixture was allowed to warm up to ambient temperature. After stirring for 10 h, removal of the solvent in vacuo left a light yellow residue. Extraction with toluene (10 mL) and centrifugation gave a yellow solution. The yellow extract was evaporated to dryness. Recrystallization from toluene/hexane afforded a light yellow crystalline solid of **4** (136 mg, 33%).

Elemental analysis. Calc. for $C_{41}H_{69}N_2O_2Si_2Zr$: C, 64.00; H, 9.04; N, 3.64. Found: C, 63.82; H, 8.62; N, 3.35%. ^{1}H NMR (C_6D_6, 298 K): $\delta = 0.20$ (s, 18H, $SiMe_3$), 0.99 (d, $J = 11$ Hz, 2H, CH_2), 1.37 (s, 18H, ^{t}Bu), 1.48 (δ, $J = 11$ Hz, 2H, CH_2), 1.85 (s, 18H, ^{t}Bu), 3.83 (d, $J = 14$ Hz, 2H, CH_2), 5.24 (d, $J = 14$ Hz, 2H, CH_2), 5.55 (s, 2H, CH), 7.00 (s, 2H, ArH), 7.63 (s, 2H, ArH); ^{13}C{^{1}H} NMR (C_6D_6, 298 K): $\delta = 4.4$ ($SiMe_3$), 31.6 (CCH_3), 32.7 (CCH_3), 35.1 (CCH_3), 36.7 (CCH_3), 54.0 (CH_2), 60.0 (CH_2), 119.0 (NCH), 124.65 (CH), 124.73 (CH), 125.8 (C), 138.5 (C), 140.5 (C), 160.4 (C), 185.8 (C, carbene).

4.3. Crystallography

Crystallographic data are summarized in Table 1. Single crystals for X-ray diffraction were grown from DME for $[H_3L]Br$ (colorless crystals), Et_2O/THF for $Na_2[L^*]$ (colorless crystals), Et_2O/hexane for $H_2[L^*]$ (colorless crystals) and **3** (light yellow crystals), toluene/hexane for **1** (colorless crystals), THF/hexane for **2** (colorless crystals). Crystals were covered in oil, and suitable single crystals were selected under a microscope and mounted on a Rigaku Mercury CCD (for H_3[L]Br, $Na_2[L^*]$, $H_2[L^*]$, and **2**) or Saturn CCD (for **1** and **3**) diffractometer equipped with a Rigaku GNNP low-temperature device. Data were collected at −100(1) °C under a cold nitrogen stream using graphite-monochromated Mo Kα radiation ($\lambda = 0.71070$ Å). The intensity images were obtained with ω scans of 0.5° interval per flame. The flame data processed using the CrystalClear (Rigaku) program, and the reflection data were corrected for absorption with a REQAB program. The structures for $Na_2[L^*]$, $H_2[L^*]$, **1** and **2** were solved by direct method, and the structures of H_3[L]Br and **3** were solved by Patterson method. These structures were refined on F^2 by the full-matrix least-squares method using CrystalStructure (Rigaku) software package [19]. For $Na_2[L^*]$ and $H_2[L^*]$, unique reflections at $2\theta < 45°$ and 50° were used for refinement due to the low quality of crystals. The hydrogen

Table 1
Crystallographic data for H_3[L]Br, Na_2[L^*], H_2[L^*], **1**, **2**, and **3**

Compound	H_3[L]Br · DME	Na_2[L^*]$_2$ · Et_2O	H_2[L]*	**1** · toluene	**2** · 6 THF	**3** · 0.5 hexane
Formula	$C_{37}H_{59}N_2O_4Br$	$C_{94}H_{150}N_4O_{11}Na_4$	$C_{33}H_{48}N_2O_2$	$C_{44}H_{62}N_2O_3Cl_2Zr$	$C_{90}H_{140}N_4O_{10}Zr$	$C_{50}H_{67}N_2O_2Zr$
Molecular weight	675.79	1604.20	504.75	829.11	1529.34	819.31
Space group	$P2_1/c$ (No. 14)	$C2/c$ (No. 15)	$P2_1/c$ (No. 14)	$P2_1/c$ (No. 14)	$P\bar{1}$ (No. 2)	$P2_1/c$ (No. 14)
a (Å)	12.316(4)	28.38(2)	13.82(1)	17.241(8)	13.4025(4)	16.240(5)
b (Å)	18.308(5)	16.14(1)	11.66(1)	13.813(6)	13.5072(1)	11.561(3)
c (Å)	17.085(5)	21.48(1)	19.88(2)	19.176(8)	26.8860(9)	24.512(8)
a (°)	90	90	90	90	76.450(7)	90
b (°)	96.799(4)	95.848(8)	103.41(1)	103.027(9)	89.583(9)	104.961(4)
g (°)	90	90	90	90	68.959(6)	90
V (Å^3)	3824(1)	9787(10)	3115(4)	4449(3)	4400.3(2)	4446(2)
Z	4	4	4	4	2	4
D_{calc} (g cm^{-3})	1.173	1.089	1.076	1.238	1.154	1.224
μ(Mo Ka) (cm^{-1})	11.149	0.846	0.659	4.049	1.815	2.869
Collected reflections	30730	39071	25215	17784	35776	35532
Unique reflections	8499	11197	7112	8917	19338	10498
Parameters	457	555	348	488	1020	541
R_1 [$I > 2s(I)$]	0.054	0.094	0.095	0.083	0.072	0.075
wR_2 (all)	0.171	0.287	0.261	0.199	0.163	0.088
Goodness-of-fit	1.001	1.013	0.974	0.990	1.069	0.985
Largest residual peak and hole (e Å^{-3})	1.51 and −0.61	2.66 and −1.16	0.99 and −0.79	6.96 and −4.31	3.12 and −2.20	1.31 and −0.85

atoms of the hydroxyl groups and the imidazolium protons for H_3[L]Br and the hydroxyl groups for H_2[L^*] were located and were refined isotropically. Anisotropic refinement was applied to all non-hydrogen atoms except for disordered atoms and crystal solvent molecules. The other hydrogen atoms were put at calculated positions with C–H distances of 0.97 Å.

5. Supplementary data

Crystallographic data for the structural analyses have been deposited with the Cambridge Crystallographic Data Center, CCDC Nos. 299115, 299116, 299117, 299118, 299119, and 299120 for compounds H_3[L]Br, Na_2[L^*], H_2[L^*], **1**, **2**, and **3**, respectively. Copies of this information may be obtained free of charged from The Director, CCDC, 12 Union Road, Cambridge CB21EZ, UK (fax: +44 1223 336 033; or e-mail: deposit@ccdc.cam.ac.uk).

Acknowledgements

Institute for Molecular Science (IMS) is thanked for financial support. This work was also supported by a Grant-in-Aid for Scientific Research [Nos. 14703008, 16655025, 17350031, and 14078101 (Priority Areas "Reaction Control of Dynamic Complexes")] from Ministry of Education, Culture, Sports, Science, and Technology, Japan.

References

[1] (a) W.A. Herrmann, Angew. Chem., Int. Ed. 41 (2002) 1290;
(b) M. Regitz, Angew. Chem., Int. Ed. Engl. 35 (1996) 725;
(c) C.M. Crudden, D.P. Allen, Coord. Chem. Rev. 248 (2004) 2247;
(d) E. Peris, R.H. Crabtree, Coord. Chem. Rev. 248 (2004) 2239.
[2] (a) D. Bourissou, O. Guerret, F.P. Gabbai, G. Bertrand, Chem. Rev. 100 (2000) 39;
(b) W.A. Herrmann, C. Köcher, Angew. Chem., Int. Ed. Engl. 36 (1997) 1262.
[3] (a) Melanie S. Sanford, Jennifer A. Love, Robert H. Grubbs, J. Am. Chem. Soc. 123 (2001) 6543;
(b) T. Weskamp, F.J. Kohl, W. Hieringer, D. Gleich, W.A. Herrmann, Angew. Chem., Int. Ed. 38 (1999) 2416;
(c) D.S. McGuinness, K.J. Cavell, B.W. Skelton, A.H. White, Organometallics 18 (1999) 1596;
(d) V. César, S. Bellemin-Laponnaz, L.H. Gade, Chem. Soc. Rev. 33 (2004) 618.
[4] (a) J.C. Green, R.G. Scurr, P.L. Arnold, F.G.N. Cloke, Chem. Commun. (1997) 1963;
(b) J. Huang, H.J. Schanz, E.D. Stevens, S.P. Nolan, Organometallics 18 (1999) 5375;
(c) R. Dorta, E.D. Stevens, C.D. Hoff, S.P. Nolan, J. Am. Chem. Soc. 125 (2003) 10490.
[5] (a) W.A. Herrmann, K. Öfele, M. Elison, F.E. Kühn, P.W. Roesky, J. Organomet. Chem. 480 (1994) C7;
(b) M. Niehues, G. Erker, G. Kehr, P. Schwab, R. Fröhlich, O. Blacque, H. Berke, Organometallics 21 (2002) 2905;
(c) N. Kuhn, T. Kratz, D. Bläser, R. Boese, Inorg. Chim. Acta 238 (1995) 179;
(d) H. Nakai, X. Hu, L.N. Zakharov, A.L. Rheingold, K. Meyer, Inorg. Chem. 43 (2004) 855;
(e) D. Pugh, J.A. Wright, S. Freeman, A.A. Danopoulos, Dalton Trans. (2006) 775.
[6] D.S. McGuinness, V.C. Gibson, J.W. Steed, Organometallics 23 (2004) 6288.
[7] (a) P.L. Arnold, S.A. Mungur, A.J. Blake, C. Wilson, Angew. Chem., Int. Ed. 42 (2003) 5981;
(b) P.L. Arnold, A.J. Blake, C. Wilson, Chem. Eur. J. 11 (2005) 6095.
[8] (a) S.A. Mungur, S.T. Liddle, C. Wilson, M.J. Sarsfield, P.L. Arnold, Chem. Commun. (2004) 2738;
(b) P.L. Arnold, S.T. Liddle, Chem. Commun. (2005) 5638;
(c) S.T. Liddle, P.L. Arnold, Organometallics 24 (2005) 2597;
(d) P.L. Arnold, S.T. Liddle, Organometallics 25 (2006) 1845;
(e) L.P. Spencer, S. Winston, M.D. Fryzuk, Organometallic 23 (2004) 3372;
(f) L.P. Spencer, M.D. Fryzuk, J. Organomet. Chem. 690 (2005) 5788.
[9] P.L. Arnold, M. Rodden, C. Wilson, Chem. Commun. (2005) 1743.
[10] S.P. Downing, A.A. Danopoulos, Organometallics 25 (2006) 1337.

[11] (a) T. Matsuo, H. Kawaguchi, Chem. Lett. 33 (2004) 640;
(b) T. Matsuo, H. Kawaguchi, J. Am. Chem. Soc. 127 (2005) 17198;
(c) F. Akagi, T. Matsuo, H. Kawaguchi, J. Am. Chem. Soc. 127 (2005) 11936;
(d) T. Matsuo, H. Kawaguchi, Organometallics 22 (2003) 5379.
[12] H. Aihara, T. Matsuo, H. Kawaguchi, Chem. Commun. (2003) 2204.
[13] A. Chandrasekaran, N.V. Timosheva, R.O. Day, R.R. Holmes, Inorg. Chem. 42 (2003) 3285.
[14] (a) C. Boehler, D. Stein, N. Donati, H. Gruetzmacher, New J. Chem. 26 (2002) 1291;
(b) B. Cetinkaya, E. Cetinkaya, J.A. Chamizo, P.B. Hitchcock, H.A. Jasim, H. Küçükbay, M.E. Lappert, J. Chem. Soc., Perkin Trans. 1 (1998) 2047;
(c) S. Solé, H. Gornitzka, O. Guerret, G. Bertrand, J. Am. Chem. Soc. 120 (1998) 9100.
[15] M. Niehues, G. Kehr, G. Erker, B. Wibbeling, R. Fröhlich, O. Blacque, H. Berke, J. Organomet. Chem. 663 (2002) 192.
[16] (a) S.L. Latesky, A.K. McMullen, G.P. Niccolai, I.P. Rothwell, J.C. Huffman, Organometallics 4 (1985) 902;
(b) C. Pellecchia, A. Grassi, A. Immirzi, J. Am. Chem. Soc. 115 (1993) 1160.
[17] (a) S. Gründemann, M. Alnrecht, J.A. Loch, J.W. Faller, R.H. Crabtree, Organometallics 20 (2001) 5485;
(b) S. Fokken, T.O. Spaniol, J. Okuda, Organometallics 16 (1997) 4240.
[18] P.H.M. Budzellar, GNMR for Windows version 4.1, Cherwell Scientific Ltd., Oxford, UK, 1999.
[19] (a) Crystal Structure Analysis Package, Rigaku and MSC, 2001;
(b) D.J. Watkin, C.K. Prout, J.R. Carruthers, P.W. Betteridge, Chemical Crystallography Laboratory, Oxford, UK.